Pattern Analysis and Applications manuscript No.
(will be inserted by the editor)

Supervised texture classification: color space or texture feature selection?

A. Porebski · N. Vandenbroucke · L. Macaire

Received: 31 October 2011 / Accepted: 30 July 2012

Abstract The color of pixels can be represented in different color spaces which take into account different properties. However, no color space is well-suited to the discrimination of all texture databases and the prior determination of such a space is not easy. In this paper, we compare the performances reached by two texture classification schemes that use color spaces:

- the Single Color Space Selection (SCSS) approach, that defines a set of texture features and then selects the color space with which the texture features allow to reach the highest classification accuracy,
- the Multi Color Space Feature Selection (MCSFS) approach, that selects texture features which have been processed from images coded into different color spaces.

Experiments carried out with benchmark texture databases show that taking advantage simultaneously of the properties of several color spaces thanks to the MCSFS approach improves the rates of well-classified images with lower learning and decision processing times.

Keywords Texture classification – Color spaces – Feature selection – Co-occurrence matrix

1 Introduction

Supervised color texture classification is a particular problem of color image retrieval. A lot of color texture classification methods have been proposed and some studies have been carried out in order to experimentally compare the performances of these methods [1,2]. For this purpose, the tested color texture classification schemes are applied to benchmark texture image datasets. One divides the images of each color texture class into the training and validation image sub-sets. The training sub-set is used to determine the parameters of the classifier during the supervised learning stage while the validation sub-set is used to evaluate the performances of the tested classification scheme during the decision stage.

In this framework, the retrieval problem can be stated in terms of finding the training images that contain the same color texture as that represented by the validation image to be classified. Several authors have shown that taking into account both the spatial arrangement of the colors in the image and the color distribution in the color space outperforms the texture discrimination quality provided by the analysis of the gray-levels [1,2,3]. So, texture features and color information are worth combining for color texture classification (see section 2).

The colors within images are initially coded by three color components represented in the three-dimensional (R,G,B) (Red, Green, Blue) color space. They can also be coded in several other three-dimensional color spaces which take into account different physical, physiologic and psycho-visual properties [4]. For the classification purpose, texture features are processed from the so-coded color images. Each texture image is thus described by a set of color texture features and is represented by a point in the corresponding feature space. During the learning stage, the training images are projected in this feature space to build the prototypes of the different texture classes. Finally, during the decision stage, a classifier assigns each validation image to a texture class by computing its similarity with the prototypes in the feature space.

A. Porebski · N. Vandenbroucke
Laboratoire LISIC - EA 4491 - Université du Littoral Côte d'Opale - Maison de la Recherche Blaise Pascal - 50, rue Ferdinand Buisson - BP 719 - 62228 Calais Cedex - FRANCE - Tel: 33 3 21 38 85 60 - Fax: 33 3 21 38 85 05 - E-mail: porebski@lisic.univ-littoral.fr

L. Macaire
Laboratoire LAGIS - FRE CNRS 3303 - Université Lille 1 - Sciences et Technologies - Cité Scientifique - Bâtiment P2 - 59655 Villeneuve d'Ascq - FRANCE

As it is difficult to find the color space that is well-suited to the discrimination of any textures, several authors have coded colors into several color spaces [1,2,3,5,6,7,8,9,10, 11,12,13]. This color coding is integrated into texture classification schemes according to two main strategies that we propose to compare in this paper:

- the **Single Color Space Selection (SCSS) approach**, presented in section 3,
- the **Multi Color Space Feature Selection (MCSFS) approach**, detailed in section 4.

The authors who have developed the SCSS approach, consider a set of texture features and compare the classification accuracies reached by classification schemes operating with these features computed from images coded with singly considered color spaces [2,3,5,6,7,10]. This "wrapper[1]" approach looks for the color space that is the best suited to discriminate the texture classes of a given database, the texture features being retained before classification. In this paper, we show that the synthesis of these works highlights several contradictions that do not allow us to find a single color space which is well-suited to the discrimination of all color textures that can be contained by natural scene images.

To solve this problem, few works propose to combine different color spaces in order to improve the performances of color image classification or segmentation. Chindaro *et al.* have developed a color texture classification system based on a set of independent classifiers where each classifier is assigned to a specific color space [14]. In order to classify images, they fuse the labeling decisions provided by these classifiers. They conclude that combining labeling decisions provided by the analysis in different color spaces improves texture classification performances. Nanni *et al.* use a similar approach, except that the classifiers are associated with color components [13]. Since the validation image is compared to the prototypes in several feature spaces, the decision stage of these latter approaches is very time consuming and is sensitive to the fusion rules.

The approach that we have proposed in an earlier study allows to combine different color spaces while avoiding these drawbacks [15]. This MCSFS approach consists firstly in coding color texture images into several color spaces and in computing texture features from the so-coded images. Since the number of features is so high that it would decrease the quality of discrimination, we determine a feature sub-space in which the texture classes are represented by well-separated and compact clusters of points. Vandenbroucke *et al.* have developed a feature selection procedure in order to determine an hybrid color space that is well-suited to the segmentation of color images [16]. We follow this approach since it has been applied with success on different applications as soccer image analysis [17]. The most discriminating features are selected thanks to a sequential selection procedure processed during the supervised learning stage. This selection procedure is based on a "filter[2]" approach that evaluates the discrimination powers of feature sub-spaces without classifying the images. According to our knowledge, there is no satisfying criterion which allows to compare the discriminating powers of feature subspaces whose dimensions are different. We thus propose to set the dimension of the retained feature sub-space to a desired value. Once this discriminating feature sub-space has been selected, a single classifier assigns the validation images during the decision stage.

Classical SCSS schemes first define a set of texture features and then select the color space with which the texture features reach the highest classification accuracy, whereas our MSCFS scheme selects texture features that have been processed from images coded into different color spaces. In this paper, we propose to compare the performances reached by these two strategies thanks to intensive experiments carried out in section 5 with benchmark texture databases. This first deep and experimental study is a contribution to answer the question: is it more relevant to select the color spaces or the color texture features? Let us notice that this study is not restricted to the classification accuracy since a careful attention is devoted to the processing times required by the schemes implemented on a same computer and with the same software tool kit.

2 Color texture features

2.1 Introduction

A color texture image is described by a set of color texture features and is represented by a point in the corresponding feature space in order to achieve the classification. There exists a large number of available color texture features and it is well-known that the performances of the classifier depend on the retained feature space [18]. Generally, the texture features can be classified into four families [19]:

- **Structural methods** describe textures thanks to primitives or textural elements which iteratively occur according to a specific arrangement or placement rules [20].
- **Random field models**, like Markov random fields [21] or autoregressive models [22], characterize textures thanks to estimated parameters of the considered model.
- **Spatial-frequency approaches**, such as wavelet transform [5,8,10], Gabor filter [23] or discrete cosine transform [24], represent textures in the frequency domain.

[1] A wrapper approach is based on the rate of well-classified images.

[2] A filter approach only takes into account the training images and does not thus depend on the classifier decision rule.

– **Statistical approaches**, such as co-occurrence matrix [1,15,25], run-length matrix [20], sum and difference histograms [26,27] or Local Binary Patterns (LBP) [2,28], describe textures according to relationships between the color components of neighboring pixels.

Different definitions of "color texture" have been proposed in the literature depending on whether the color and the texture informations are considered jointly or separately [2,24]. According to these definitions, color textures can be characterized by:

– **luminance based texture features** coupled with color statistical features [29,30].
– "luminance based texture features" combined with "pure chrominance based texture features". The **pure chrominance based texture features** are defined as a complex function depending on two chrominance components [31].
– **within color component texture features** which take into account the spatial relationships within each of the three color components of a color space [12,24,26].
– **within and between color component texture features** which consider the spatial relationships within and between the three components of a color space [1,15,25].

Even if the first three approaches seem to be computationally fast, they do not take into account the spatial relationships between the three color components. So, the information contained in the whole color texture is lost and the classification quality can be reduced [25]. That is the reason why several authors privilege features which take into account spatial relationships both within and between the three color components [1,25,32].

In this framework, we have shown that the well-known Haralick features extracted from Reduced Size Chromatic Co-occurrence Matrices (RSCCMs) are easy to be implemented and are relevant to characterize color textures because they allow to compute within and between color component texture features [33]. That is the reason why we choose to compute these features to carry out our experimental study, although there are many other features which are also well-suited to classify color textures.

In the second part of this section, we present the RSCCMs from which are extracted Haralick features described in the third part.

2.2 Reduced size chromatic co-occurrence matrices

The Chromatic Co-occurrence Matrix (CCM), introduced by Rosenfeld [34], has been taken up by Palm as a texture descriptor extracted from a color image [1]. It is a statistical texture descriptor which takes into account both the color distribution in a color space and the spatial interactions within and between the color components of neighboring pixels. Let C_k and $C_{k'}$, be two of the three color components of a color space denoted (C_1,C_2,C_3)[3] ($k,k' \in \{1,2,3\}$) and let $M_{\mathscr{N}}^{C_k,C_{k'}}[\mathbf{I}]$, be the CCM which measures the spatial interactions in the neighborhood $\mathscr{N}$ between the color components C_k and $C_{k'}$ characterizing the pixels of the image $\mathbf{I}$. The cell $M_{\mathscr{N}}^{C_k,C_{k'}}[\mathbf{I}](i,j)$ of this matrix contains the number of times that a pixel P whose color component value $C_k(P)$ is equal to i, is the neighbor, according to the neighborhood $\mathscr{N}$, of a pixel P' whose color component value $C_{k'}(P')$ is equal to j. The neighborhood $\mathscr{N}$ is a parameter defined by the user.

As the CCM measures the local interaction between neighboring pixels, it is sensitive to significant differences of the image size. To decrease this sensitivity, we have to normalize the CCM by the total co-occurrence number. Let $m_{\mathscr{N}}^{C_k,C_{k'}}[\mathbf{I}]$, be the normalized CCM:

$$m_{\mathscr{N}}^{C_k,C_{k'}}[\mathbf{I}] = \frac{M_{\mathscr{N}}^{C_k,C_{k'}}[\mathbf{I}]}{\sum_{i=0}^{Q-1}\sum_{j=0}^{Q-1} M_{\mathscr{N}}^{C_k,C_{k'}}[\mathbf{I}](i,j)}, \quad (1)$$

where Q is the number of levels used to quantify the color components. For example, for a 24 bits true color image, Q is equal to 256.

For a given image $\mathbf{I}$ and a given neighborhood $\mathscr{N}$, $N_M = 6$ CCMs are thus computed:

– three within color component matrices denoted: $m_{\mathscr{N}}^{C_1,C_1}[\mathbf{I}]$, $m_{\mathscr{N}}^{C_2,C_2}[\mathbf{I}]$, $m_{\mathscr{N}}^{C_3,C_3}[\mathbf{I}]$,
– three between color component matrices denoted: $m_{\mathscr{N}}^{C_1,C_2}[\mathbf{I}]$, $m_{\mathscr{N}}^{C_1,C_3}[\mathbf{I}]$ and $m_{\mathscr{N}}^{C_2,C_3}[\mathbf{I}]$.

As the CCMs are symmetric, we choose only one matrix $m_{\mathscr{N}}^{C_k,C_{k'}}[\mathbf{I}]$ among the two matrices $m_{\mathscr{N}}^{C_k,C_{k'}}[\mathbf{I}]$ and $m_{\mathscr{N}}^{C_{k'},C_k}[\mathbf{I}]$, which describe the information provided by the spatial correlation between the color components C_k and $C_{k'}$.

A Reduced Size Chromatic Co-occurrence Matrix (RSCCM) is a $Q \times Q$ CCM, where Q is reduced in order to decrease the memory storage cost and so, the time required to extract texture features from these matrices. In a previous study, we have shown that when Q is set to 16, RSCCM analysis reaches satisfying classification results while significantly reducing the processing time [33].

2.3 Haralick features extracted from RSCCMs

Usually, CCMs are not directly exploited because they contain a large amount of information. In order to reduce it while preserving the relevance of these descriptors, the first $N_H = 13$ Haralick features denoted f_1 to f_{13} are extracted

[3] The notation (C_1,C_2,C_3) is a generic one for the three-dimensional color spaces.

from theses matrices [35]: homogeneity (f_1), contrast (f_2), correlation (f_3), variance (f_4), inverse difference moment (f_5), sum average (f_6), sum variance (f_7), sum entropy (f_8), entropy (f_9), difference variance (f_{10}), difference entropy (f_{11}), and two information measures of correlation (f_{12} and f_{13}).

Four 2-directional neighborhoods are usually used to compute direction-dependent co-occurrence matrices [35]. These four neighborhoods, shown in figure 1, are based on two neighbors along four different directions (0^o, 45^o, 90^o, 135^o) and on the spatial infinity-norm distance v separating the considered pixel from its neighbors. The adjustment of this distance v depends on the spatial resolution of the texture images.

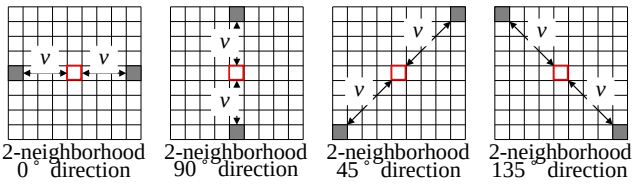

Fig. 1 2-directional neighborhoods in which neighboring pixels are labeled as gray.

For texture classification, Haralick proposes to extract texture features from four direction-dependent CCMs, computed with each of the four 2-directional neighborhoods [35]. Then, he computes the mean and the variance of the extracted features in order to be rotationally invariant.

To reduce the computation time, we propose to use another approach which consists in extracting the Haralick features from RSCCMs computed with only one neighborhood. Indeed, computing only one RSCCM instead of computing four direction-dependent ones reduces the memory storage cost and so the computation time.

To choose this neighborhood, we rely on a previous study which proves that the choice of the neighborhood shape used to compute CCM depends on the observed textures [36]. When they do not present any privileged direction, we should compute features which take into account all the possible directions. That is the reason why we choose to use the isotropic 8-neighborhood ($v = 1$), denoted $\mathscr{N} = 3 \times 3$ [12,25] (see figure 2). Using this neighborhood to compute RSCCM is equivalent to summing the four direction-dependent RSCCMs computed thanks to the four 2-directional neighborhoods presented in figure 1. It allows thus to take into account the four directions simultaneously with only one RSCCM.

After having described the color texture features used in this paper, the next section details the Single Color Space Selection (SCSS) approach.

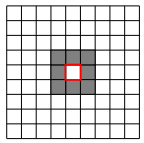

Fig. 2 Isotropic 8-neighborhood ($\mathscr{N} = 3 \times 3$).

3 Single Color Space Selection (SCSS) approach

There are many color spaces to represent the colors according to different properties (see section 3.1). However, the prior determination of a color space which is well-suited to a specific classification problem, is not easy. Many authors have thus tried to find the color space which allows to discriminate the textures as better as possible. For this purpose, they have compared the performances reached by classification approaches applied to images whose colors are coded in different color spaces which are singly considered (SCSS approach). The synthesis of these experimental comparisons is presented in section 3.2.

3.1 Color spaces

The colors of pixels can be represented in different 3-dimensional color spaces which take into account different physical, physiologic and psycho-visual properties [4]. The three color components of each color space are processed from the (R,G,B) color space thanks to different coding schemes based on linear or non-linear transformations.

Figure 3 shows several spaces commonly used in color image analysis and classified into four families [4]:

- The **primary spaces** are based on the trichromatic theory, which assumes that any color can be reproduced by the mixture of three primary colors: the red, the green and the blue. There are several (R,G,B) real primary spaces (and their normalized coordinate ones (r,g,b)) whose definition depends on the acquisition device. Each of these (R,G,B) spaces can be transformed into the single CIE[4] (X,Y,Z) virtual primary space which is device independent. Normalized coordinates (x,y,z) can also be deduced from CIE (X,Y,Z) to characterize color.
- The **luminance-chrominance spaces** are composed by one "luminance" component which represents an achromatic information and two "chrominance" components which characterize the chromatic information. These color spaces can be divided into four sub-families [4]:
  - the antagonist spaces, like $(A,C1,C2)$ and (bw,rg,by),

[4] Commission Internationale de l'Eclairage (International Commission on Illumination)

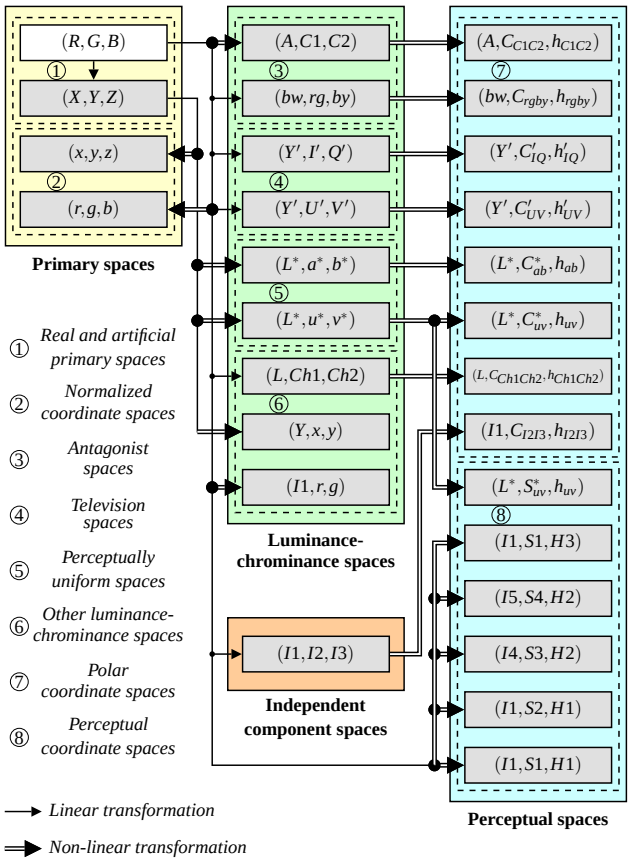

Fig. 3 Color space families (linear transformations are represented by simple arrows whereas non-linear ones are represented by double arrows).

- the television spaces, like (Y',I',Q'), (Y',U',V') and (Y,Cb,Cr),
- the CIE perceptually uniform spaces, like (L^*,a^*,b^*), (L^*,u^*,v^*) and (U,V,W),
- and the other luminance-chrominance spaces, like $(I1,r,g)$, (L,U,V), CIE (Y,x,y) and the Carron's $(L,Ch1,Ch2)$ color space [4].

The three components of luminance-chrominance spaces are derived from the (R,G,B) components by linear or non-linear transformations, depending on the type of luminance-chrominance spaces: the components of television spaces and some antagonist spaces are obtained thanks to linear transformations of the (R,G,B) components, whereas the components of CIE perceptually uniform spaces are derived from the (R,G,B) components by non-linear transformations.

– The **independent axis spaces** result from different statistical methods, like PCA (Principal Component Analysis), which provide as less correlated components as possible. In this paper, we use the well-known $(I1,I2,I3)$ color space proposed by Ohta [37].
– The **perceptual spaces** attempt to quantify the subjective human color perception by using the intensity, the hue and the saturation components. Two kinds of perceptual spaces can be distinguished:
  - The polar coordinate spaces correspond to expressions in polar coordinates of the luminance-chrominance components. Here, we consider (A,C_{C1C2},h_{C1C2}), $(L,C_{Ch1Ch2},h_{Ch1Ch2})$, (bw,C_{rgby},h_{rgby}), (Y',C'_{IQ},h'_{IQ}), (Y',C'_{UV},h'_{UV}), (L^*,C^*_{ab},h_{ab}), (L^*,C^*_{uv},h_{uv}) and $(I1,C_{I2I3},h_{I2I3})$, which are derived from the previously mentioned luminance-chrominance spaces.
  - The perceptual coordinate spaces are directly deduced from primary spaces. Among many available coordinate spaces, we use in this paper the $(I1,S2,H1)$ triangle space, the $(I1,S1,H1)$ modified triangle space (which is commonly denoted HSI), the $(I4,S3,H2)$ hexcone space (which is commonly denoted HSV), the $(I5,S4,H2)$ double hexcone space (which is commonly denoted HLS), the $(I1,S1,H3)$ Liang space and the CIE (L^*,S^*_{uv},h_{uv}) space.

  Let us note that perceptual spaces can also be considered as luminance-chrominance ones because they are composed of one luminance component and two chrominance ones.

Once the three components of a color space have been processed from the (R,G,B) ones by linear or non-linear transformations, they are rounded, scaled and normalized to range between the unsigned integer values 0 and $Q-1$ (Q is the number of levels used to quantify the color components), thanks to a coding scheme which takes into account the properties of the different color spaces [4].

3.2 Single Color Space Selection (SCSS) approach

The Single Color Space Selection (SCSS) approach looks for the color space with which the rate of well-classified validation images is the highest. First, it retains a set of texture features. Then, it compares the classification performances reached with these features extracted from images coded in different color spaces which are singly considered. This wrapper approach that does not select any feature, has been followed by several authors [2,6,7,10,24], as shown in table 1.

The first column of this table indicates the references of the works which have developed a SCSS approach. The second one presents the color spaces that have been used to code the colors within the images. The texture features which have been processed from the color images, are shown in the third column. The classifier and the database used to measure the classification accuracy are presented in the fourth and the fifth columns, respectively. Finally, the last column shows the color space which provides the high-

Table 1 Best suited color spaces determined by SCSS approaches (1-NN and SVM means that the one Nearest Neighbor classifier and the Support Vector Machines classifier are performed, respectively. Please refer to [38] for a detailed discussion on the computation of the non-linear-(R,G,B) and the *sRGB* color spaces).

Ref.	Color spaces	Texture features	Classifier	Data-base	Best suited color space
[2]	(R,G,B) (r,g,b) (L^*,a^*,b^*) $(I1,I2,I3)$ $(I4,S3,H2)$	3D color histograms	1-NN	OuTex	$(I4,S3,H2)$
				VisTex	$(I1,I2,I3)$
		LBP histograms	1-NN	OuTex	(R,G,B)
				VisTex	(L^*,a^*,b^*)
		Features from Gabor transform	1-NN	OuTex	(R,G,B)
				VisTex	(L^*,a^*,b^*)
[7]	(R,G,B) (L^*,a^*,b^*) $(I1,I2,I3)$ $(I4,S3,H2)$	LBP histograms	SVM	OuTex	$(I4,S3,H2)$
				VisTex	(R,G,B) $(I4,S3,H2)$ $(I1,I2,I3)$
		LBP histograms + contrast feature	SVM	OuTex	$(I4,S3,H2)$
				VisTex	(R,G,B)
		Features from wavelet transform	SVM	OuTex	(L^*,a^*,b^*)
				VisTex	$(I1,I2,I3)$
[6]	(R,G,B) non-linear-(R,G,B) *sRGB* (X,Y,Z) (L^*,a^*,b^*) (L^*,u^*,v^*) $(I1,I2,I3)$ (Y,Cb,Cr) (Y',I',Q') (L^*,C^*_{ab},h_{ab}) (L^*,C^*_{uv},h_{uv})	Color moments + correlogram features	k-NN	VisTex	(L^*,a^*,b^*)
[24]	(R,G,B) (X,Y,Z) (L^*,a^*,b^*) (H,S,I) (Y',I',Q')	Features from discrete cosine transform	Neural network	VisTex	(Y',I',Q')
[10]	(R,G,B) (Y,Cb,Cr) $(I5,S4,H2)$	Features from wavelet transform	3-NN	VisTex	(R,G,B)

est accuracy for the considered application. Let us note that we present in this table the works which have been applied to Outex and VisTex benchmark color texture databases [39, 40].

For example, Mäenpää *et al.* propose to code the colors within the images in five different color spaces ((R,G,B), (r,g,b), (L^*,a^*,b^*), $(I1,I2,I3)$ and $(I5,S4,H2)$). From these images, they compute 3D color histograms, which constitute the feature space in which the Nearest Neighbor (1-NN) classifier operates. Mäenpää *et al.* conclude that the $(I5,S4,H2)$ perceptual space is the best suited to the discrimination of the Outex color textures [2].

The synthesis of these experimental comparisons shows that the choice of the best color space depends on different parameters. Indeed, let us focus on the studies [2] and [7]:

- First, Mäenpää *et al.* show that the choice of the most discriminating color space depends on the considered color texture database. For example, they use the LBP histograms analyzed by the 1-NN classifier to discriminate the different color texture classes of the Outex and VisTex databases. They show that the VisTex texture images are better classified with the (L^*,a^*,b^*) color space (99.3%) than with the (R,G,B) space (97.9%). This order is inverted for the Outex texture database, for which the rates of well-classified images reach 87.8% with the (R,G,B) space and 82.9% by considering the (L^*,a^*,b^*) color space. Let us note that these experimental results also show that the color space can strongly modify the accuracy.
- The most discriminating color space can also depends on the used texture features [6, 24, 10]. For example, depending on whether the color textures are characterized by LBP histograms or features extracted from wavelet transform, Iakovidis *et al.* conclude in a different way about the color space which is the best suited to discriminate the textures of the Outex database thanks to SVM scheme [7]. When LBP histograms are considered, they show that the $(I4,S3,H2)$ perceptual color space allows to obtain better classification accuracy (93.5%) than the one reached thanks to the (L^*,a^*,b^*) space (91.5%). On the other hand, when features extracted from wavelet transform are used to build the feature space, the most discriminating color space is (L^*,a^*,b^*) (89.7%), which allows to improve the classification results obtained with the $(I4,S3,H2)$ space (89%).

Finally, the synthesis of these experimental comparisons does not allow us to conclude on the definition of a single color space which is well-suited to the discrimination of all texture databases, whatever the considered texture features. Moreover, experiments done by Mäenpää *et al.* have revealed that the choice of the color space is crucial for the color texture classification applications where the classification accuracy is the main objective. However, the prior determination of a color space which is well-suited to the discrimination of the considered color texture classes is not easy. The MCSFS approach attempts to solve this problem.

4 Multi Color Space Feature Selection (MCSFS) approach

Rather than looking for the best color space, the Multi Color Space Feature Selection (MCSFS) approach selects color texture features. For this purpose, it first codes the colors of texture images into several color spaces [15]. Then, candidate color texture features are computed from the so-coded images (see section 4.1). As their number can be very high, they are selected thanks to a supervised feature selection procedure in order to build a low dimensional discriminating feature sub-space in which a classifier operates (see section 4.2).

4.1 Candidate color texture features

In order to exploit the properties of several color spaces, each image is first coded in each of the $N_S = 28$ color spaces described in section 3.1. For this purpose, the color components of each image, initially coded in the (R,G,B) acquisition color space, are converted to color components of each of the 28 color spaces of figure 3 thanks to linear or non-linear transformations [4]. Then, the $N_M = 6$ RSCCMs are computed from the so-coded images and the $N_H = 13$ Haralick features are extracted from each matrix (see section 2).

A color texture is thus represented by $N_f = N_S \times N_M \times N_H$ candidate color texture features denoted X_l $(l = 1,\ldots,N_f)$ as displayed by figure 4.

Different sub-sets of candidate features can be constituted. Each of them corresponds to a candidate feature sub-space which takes into account the properties of several color spaces. However, it is well-known that the performance of a classifier, in terms of rates of well-classified images, depends on the dimension of the feature sub-space due to the curse of dimensionality [18]. To reach satisfying classification accuracies and also decrease the computation time, we have to reduce the number of color texture features by selecting the most discriminating ones. The next section details the feature selection procedure performed by the MCSFS approach.

4.2 Supervised feature selection

The proposed feature selection scheme, based on a "filter" strategy, consists in selecting during the learning stage a D-dimensional discriminating feature sub-space, in which the classifier operates during the decision stage.

The selection of a feature sub-space requires both a sub-space search algorithm and an evaluation function that measures the quality of the sub-spaces.

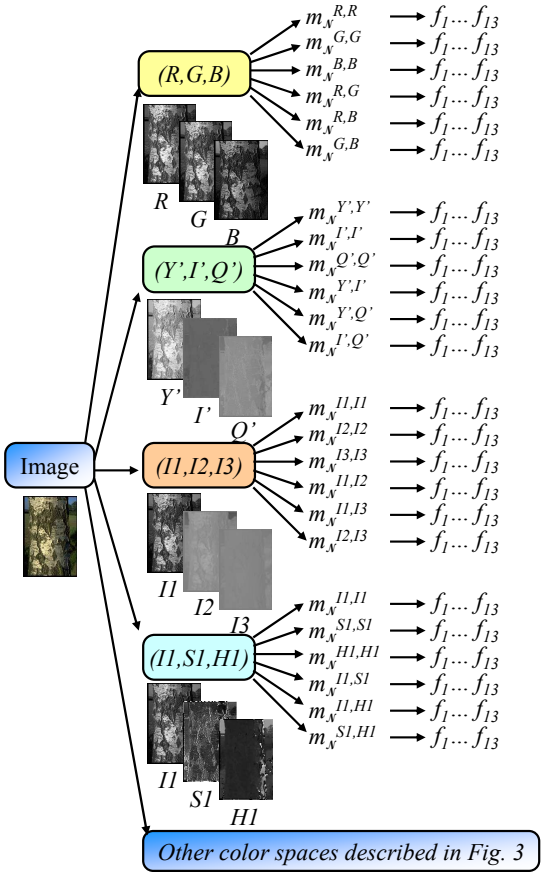

Fig. 4 Candidate color texture features.

4.2.1 Sub-space search algorithm

The selection of the D-dimensional feature sub-space can be achieved thanks to several non-exhaustive iterative selection procedures, such as SFS (Sequential Forward Selection), SBS (Sequential Backward Selection), SFFS (Sequential Forward Floating Selection) or SBFS (Sequential Backward Floating Selection) [41]. The number N_f of candidate color texture features being high, we choose to process a forward procedure, where candidate features are iteratively added from an empty set. Once we have compared the performances of SFS and SFFS procedures in terms of classification results and computation time, we have experimentally shown that the SFS procedure allows to obtain similar color texture classification accuracies than those obtained with the SFFS one, while significantly reducing the processing time [42]. That is the reason why we choose the SFS procedure to build the D-dimensional feature sub-space.

At each step of this SFS procedure, an informational criterion J is evaluated in order to measure the discriminating power of each candidate feature sub-space. At the beginning of this procedure, the N_f one-dimensional candidate feature

sub-spaces, defined by each of the N_f candidate color texture features, are examined. The candidate feature which minimizes (or maximizes, depending on the considered evaluation function) J is selected at the first step. In the second step of the procedure, this selected feature is associated with each of the (N_f-1) remaining candidate color texture features in order to constitute (N_f-1) two-dimensional candidate feature sub-spaces. We consider that the two-dimensional sub-space that minimizes (or maximizes) J is the best two-dimensional sub-space for discriminating the color texture classes...

The pseudo code of the SFS algorithm is described in figure 5:

- The initial inputs of this algorithm are the set $\mathscr{E}$ of the N_f candidate features X_l ($l=1,\ldots,N_f$) and the dimension D of the selected sub-space. The outputs are the d-dimensional feature sub-spaces $\mathscr{E}_d$ ($d=1,\ldots,D$) and particularly the D-dimensional selected feature sub-space $\mathscr{E}_D$.
- As the sequential selection procedure is a "Forward" type algorithm, the evaluated feature sub-space is initially empty ($\mathscr{E}_0=\varnothing$).
- At each step d of the SFS procedure, we consider the (N_f-d) feature sub-spaces $\mathscr{E}_d\cup\{X_l\}$, composed of the d features that have been already selected and of one of the available features X_l (the available features are those which have not been yet selected, i.e. those which belong to the sub-space $\mathscr{E}\backslash\mathscr{E}_d$). The discriminating power $J(\mathscr{E}_d\cup\{X_l\})$ of each of these sub-spaces is then evaluated. The feature X_l which minimizes (or maximizes) $J(\mathscr{E}_d\cup\{X_l\})$ is associated with the sub-space $\mathscr{E}_d$ of the already selected features in order to constitute the $(d+1)$-dimensional feature sub-space $\mathscr{E}_{d+1}$. The value of d is then incremented ($d=d+1$).
- Once the D-dimensional sub-space has been determined, the selection procedure stops.

Among the candidate features belonging to the sub-space $\mathscr{E}\backslash\mathscr{E}_d$, some are more or less correlated to the d already selected features. Arvis *et al.* have shown that looking for uncorrelated features yields satisfying results [25]. In order to only select color texture features which are correlated as less as possible, we measure the correlation level between each of the candidate color texture features and each of the $(d-1)$ features that have been already selected. The candidate feature is examined only if its correlation level is lower than a threshold fixed by the user (here, 75%) [16].

4.2.2 Evaluation function

The discriminating power $J(\mathscr{E}_d\cup\{X_l\})$ of each sub-space is estimated with the training images. A color texture image is characterized in a feature sub-space by a point whose coordinates are the values of the color texture features defining this sub-space. So, the images corresponding to a color texture class give rise to a cluster of points in this feature sub-space. We assume that the more the clusters associated with the different color texture classes are well-separated and compact in the feature sub-space, the higher the discriminating power of this feature sub-space is. That leads us to choose a measure of class separability and compactness as evaluation function. There are several measures, like Wilks's criterion, Trace criterion or Hotelling ones, for which we have experimentally shown that the corresponding classification performances are similar [42]. So, we choose the Wilks's criterion, which has to be minimized [43]:

$$J=\frac{|\Sigma_W|}{|\Sigma_W+\Sigma_B|}, \tag{2}$$

where Σ_W is the within-class dispersion matrix which characterizes the compactness of each color texture class, Σ_B is the between-class dispersion matrix which measures the class separability between the different classes and $|\Sigma|$ is the determinant of the matrix Σ.

When the clusters of points in the considered feature sub-space are well-separated and compact, J is close to 0. On the other hand, when the points are scattered in the feature sub-space and the clusters corresponding to different texture classes overlap, J is high.

At each step d of the sequential selection procedure, a feature is added and the criterion J increases with the dimension of the selected feature sub-space. So, we cannot compare the criterion J for feature sub-spaces with different dimensions. As this criterion does not allow to determine the best dimension of the feature sub-space, we choose to fix the parameter D to 40 for our experiments. This value has been experimentally chosen after having analyzed the classification results obtained with different color texture sets in a

Input
$\mathscr{E}=\{X_l \mid l=1,\ldots,N_f\}$, the N_f candidate features,
D, the dimension of the selected sub-space.
Output
$\mathscr{E}_d=\{Y_k\in\mathscr{E} \mid k=1,\ldots,d\}$, the d-dimensional feature sub-spaces ($d=1,\ldots,D$).
Initialization

$d=0$;
$\mathscr{E}_0=\varnothing$;
Do

$Y_{d+1}=\underset{X_l\in\mathscr{E}\backslash\mathscr{E}_d}{\operatorname{argmin}} \; J(\mathscr{E}_d\cup\{X_l\})$;
$\mathscr{E}_{d+1}=\mathscr{E}_d\cup\{Y_{d+1}\}$;
$d=d+1$;
While $d<D$

Fig. 5 SFS Algorithm.

previous study. It shows that the rates of well-classified images generally increase with respect to the dimension d of the selected feature sub-space and are stabilized when d is higher than or equal to 40 [42]. Obviously, this value should be adjusted depending on the considered application.

Once the D-dimensional discriminating color texture feature sub-space has been selected, a classifier assigns the validation images during the decision stage. Many classifiers (k-NN, Neural Networks, SVM,...) have been used to classify color texture images [7,26]. We choose to classify the images of the validation sub-set thanks to the simple and widely used 1-NN classifier since it requires no parameter.

After having described the SCSS and MCSFS approaches, we propose to compare the performances reached by these two strategies thanks to intensive experiments carried out in the next section.

5 Experiments

In order to compare the performances reached by the proposed MCSFS approach with regard to those cited in previous works, the experiments are achieved with two texture sets coming from two well-known and largely used benchmark color texture databases (see section 5.1).

First, we propose to measure the influence of the color space choice on the color texture classification results reached by a SCSS approach (see section 5.2). Then, we present the experimental results obtained by the MCSFS approach (see section 5.3) and compare its performances with those obtained by SCSS texture classification schemes (see section 5.4). An analysis of the processing times required by the learning and the decision stages is finally presented in section 5.5.

5.1 Color texture databases

Outex and VisTex are two well-known color texture databases. Different sets coming from these databases have been proposed in order to experiment and compare the performances reached by color texture classification approaches. In this section, we present two texture sets, coming from Outex and VisTex databases respectively, used to carry out our experiments [39,40].

5.1.1 Outex database

Outex contains a very large number of surface textures acquired under controlled conditions by a 3-CCD digital color camera. These textures are split up into 29 categories of color texture images like wood, fabric, wallpaper, sand, tile, ... The number of images by category ranges from 1 to 47 according to the considered category. The images of Outex database are acquired under three different illuminants (a 2300 K horizon sunlight source, a 2856 K incandescent CIE A light source and a 4000 K fluorescent source), six different resolutions (100, 120, 300, 360, 500 and 600 dpi) and nine different rotation angles (0 °, 5 °, 10 °, 15 °, 30 °, 45 °, 60 °, 75 ° and 90 °) [39].

To build the Outex set[5], 68 color texture images of this database, whose size is 746×538 pixels, are split up into 20 disjoint sub-images whose size is 128×128 pixels [2]. Here, the 20 sub-images of a same class thus come from the same acquired image. Figure 6 illustrates the used Outex set where each class of this set is represented by one image.

Fig. 6 68 Outex color textures: each image represents a class of texture.

Let us note that several of these color texture images come from the same category of color textures but each of the 68 images defines one class of color texture. So, the discrimination between the different classes by a visual examination of the images is not always easy, particularly for the last eleven classes which all represent rice textures (see figure 6).

The images of the considered Outex set have been acquired with a 100 dpi resolution at 0^o rotation and with the 2856 K incandescent CIE A light source. The transformation matrix, which converts the R, G and B component levels to the CIE X, Y and Z ones, is given by [2]:

$$\begin{bmatrix} X \\ Y \\ Z \end{bmatrix} = \begin{bmatrix} 0.9176 & 0.1242 & 0.0550 \\ 0.6690 & 0.3165 & 0.0145 \\ 0.0013 & 0.0475 & 0.3068 \end{bmatrix} \begin{bmatrix} R \\ G \\ B \end{bmatrix}. \quad (3)$$

[5] The Outex set is available at the Outex web site as test suite Outex-TC-00013 (`http://www.outex.oulu.fi/temp/`).

Among the 1360 images of the Outex set, 680 images are used to build the training sub-set and the 680 remaining ones to build the validation sub-set, according to the holdout method.

We choose this set because it is one of the most often used by other authors [2,7,25,44]. As the authors who have experimented their works on this set do, we analyze the performances of our classification scheme thanks to the rates of well-classified validation images.

5.1.2 VisTex database

In order to apply our scheme to the discrimination of natural color textures observed under non-controlled illumination conditions, we consider the VisTex database [40]. To build the VisTex set[6], 54 color texture images (see figure 7), whose size is 512×512 pixels, are split up into 16 disjoint sub-images whose size is 128×128 pixels [2]. So, the 16 sub-images of a same class come from the same acquired image.

Fig. 7 54 VisTex color textures: each image represents a class of texture.

Because no information is given about the acquisition conditions of the textures of this database, the corresponding images can not be coded into color spaces requiring to know this information, like the spaces derived from the (X,Y,Z) space.

Among the 864 images of the VisTex set, 432 images are used to build the training sub-set and the 432 remaining ones to build the validation sub-set, according to the holdout decomposition.

As for the Outex set, we choose to use the VisTex set since it is the most often used by works of other authors [2,7, 25,44]. In order to compare our results with these works, we also analyze the performances of our classification scheme thanks to the rates of well-classified validation images.

After having described the two color texture sets used to carry out our experiments, experimental results achieved with the SCSS approach are firstly described in the next section.

5.2 Color space choice and color texture classification accuracy

The prior choice of a color space which is well-suited to the discrimination of the considered classes is a challenging problem. Indeed, it depends on the computed texture features and on the classifier. In order to illustrate the influence of the color space choice on color texture classification accuracy, we propose to measure the performances obtained by the SCSS approach, i.e. by using independently different color spaces.

For the Outex set, we consider each of the $N_S = 28$ color spaces shown in figure 3. However, since the textures of the VisTex set are observed under uncontrolled illumination conditions, we don't know the transformation matrix which converts the R, G and B component levels to the X, Y and Z ones. That is the reason why we retain only $N_S = 20$ color spaces out of the 28 presented in figure 3, removing thereby the (X,Y,Z) space and those which are computed from it (i.e. (x,y,z), (L^*,a^*,b^*), (L^*,u^*,v^*), (Y,x,y), (L^*,C^*_{ab},h_{ab}), (L^*,C^*_{uv},h_{uv}) and (L^*,S^*_{uv},h_{uv})).

For each color space, $N_f = 13$ Haralick features $\times 6$ RSCCMs $= 78$ candidate color texture features are computed. The 1-NN classifier thus operates in a 78-dimensional feature space to discriminate the different texture classes.

Tables 2 and 3 show the color space sorted in descending order according to the rate T of well-classified validation images obtained thanks to the SCSS approach, for the Outex and VisTex sets respectively.

The rank of each color space is shown in the first column of these tables. The corresponding color space and its family (see figure 3) are presented in the second and the third columns, respectively, and the last column shows the rate T of well-classified validation images obtained by coding colors with each color space.

By examining these tables, we notice that the (R,G,B) color space (and the primary spaces in general) is not the space which provides the best results. So, considering other color spaces improves the texture classification accuracy. These tables also show that extracting features from images coded in the perceptual spaces allows generally to obtain very satisfying classification performances whatever the considered database. Particularly, for the Outex set, the highest classification accuracy ($T = 92.5\%$) is obtained thanks to the $(I5,S4,H2)$ (i.e. HLS) perceptual space. On the other

[6] The VisTex set is available at the Outex web site as test suite Contrib-TC-00006 (`http://www.outex.oulu.fi/temp/`).

Table 2 Color space ranking according to the classification accuracy T obtained with the Outex validation sub-set.

Rank	Color space	Color space family	T (%)
1	$(I5,S4,H2)$	Perceptual	92.5
2	$(I1,C_{I2I3},h_{I2I3})$	Perceptual	91.6
3	(R,G,B)	Primary	91.5
4	$(I1,S2,H1)$	Perceptual	91.3
5	$(I1,r,g)$	Luminance-chrominance	91.2
6	$(I1,S1,H3)$	Perceptual	91.0
7	$(I4,S3,H2)$	Perceptual	90.9
7	$(I1,S1,H1)$	Perceptual	90.9
7	(bw,C_{rgby},h_{rgby})	Perceptual	90.9
7	(Y',C'_{IQ},h'_{IQ})	Perceptual	90.9
11	$(L,C_{Ch1Ch2},h_{Ch1Ch2})$	Perceptual	90.7
12	(Y',C'_{UV},h'_{UV})	Perceptual	90.6
13	(A,C_{C1C2},h_{C1C2})	Perceptual	90.3
14	(L^*,C^*_{uv},h_{uv})	Perceptual	90.2
15	(bw,rg,by)	Luminance-chrominance	89.7
16	$(I1,I2,I3)$	Independent component	89.4
17	(Y',U',V')	Luminance-chrominance	89.1
18	(L^*,C^*_{ab},h_{ab})	Perceptual	89.0
18	(Y',I',Q')	Luminance-chrominance	89.0
20	$(L,Ch1,Ch2)$	Luminance-chrominance	88.8
21	(L^*,S^*_{uv},h_{uv})	Perceptual	88.7
22	(X,Y,Z)	Primary	87.2
23	(L^*,a^*,b^*)	Luminance-chrominance	87.1
24	(L^*,u^*,v^*)	Luminance-chrominance	86.9
25	$(A,C1,C2)$	Luminance-chrominance	85.4
26	(Y,x,y)	Luminance-chrominance	84.9
27	(r,g,b)	Primary	80.7
28	(x,y,z)	Primary	69.0

Table 3 Color space ranking according to the classification accuracy T obtained with the VisTex validation sub-set.

Rank	Color space	Color space family	T (%)
1	$(L,Ch1,Ch2)$	Luminance-chrominance	99.3
2	$(I4,S3,H2)$	Perceptual	98.8
3	$(I1,S2,H1)$	Perceptual	98.6
3	$(I1,S1,H1)$	Perceptual	98.6
3	(Y',C'_{UV},h'_{UV})	Perceptual	98.6
3	(Y',I',Q')	Luminance-chrominance	98.6
3	$(I1,I2,I3)$	Independent component	98.6
8	$(I1,C_{I2I3},h_{I2I3})$	Perceptual	98.4
8	(bw,C_{rgby},h_{rgby})	Perceptual	98.4
8	(Y',C'_{IQ},h'_{IQ})	Perceptual	98.4
11	$(I1,S1,H3)$	Perceptual	97.9
11	$(I5,S4,H2)$	Perceptual	97.9
13	$(L,C_{Ch1Ch2},h_{Ch1Ch2})$	Perceptual	97.7
14	(bw,rg,by)	Luminance-chrominance	97.5
15	(A,C_{C1C2},h_{C1C2})	Perceptual	97.2
16	(Y',U',V')	Luminance-chrominance	97.0
17	$(I1,r,g)$	Luminance-chrominance	96.8
18	$(A,C1,C2)$	Luminance-chrominance	96.8
19	(r,g,b)	Primary	94.4
20	(R,G,B)	Primary	94.2

hand, for the VisTex database, the color space with the highest classification accuracy ($T = 99.3\%$) is the Carron's $(L,Ch1,Ch2)$ luminance-chrominance space.

According to the considered color space, the difference between the maximum and the minimum classification accuracies can reach nearly 24% (23.5% for the Outex set and 5.1% for the VisTex set). The classification performances thus strongly depend on the color space in which the colors are coded. However, the classification accuracies obtained with perceptual color spaces are globally high with a low dispersion. Indeed, the variation reaches 3.8% for the Outex set (with the best rate of well-classified images) and 2.1% for the VisTex set.

These experiments show the importance of the color space choice for color texture classification purposes.

Rather than defining the texture features and selecting the best color space, we propose to select the best texture features computed with several color spaces thanks to the MCSFS approach described in the next section.

5.3 Multi Color Space Feature Selection

The MCSFS approach analyzes Haralick features extracted from RSCCMs computed from images coded in N_S different color spaces. As explained in the previous section, we consider the $N_S = 28$ color spaces of figure 3 for the Outex set. The number of candidate color texture features considered for this set is thus $N_f = 13 \times 6 \times 28 = 2184$ as previously explained. For the VisTex set, the color spaces depending on the (X,Y,Z) space are not taken into account. $N_S = 20$ color spaces are thus considered, that makes a number of candidate color texture features N_f equal to $13 \times 6 \times 20 = 1560$.

Among the N_f candidate color texture features, the MCSFS approach sequentially selects the most discriminating ones in order to build a feature sub-space whose dimension D is equal to 40. The first ten features selected by this MCSFS approach are shown by tables 4 and 5, for the Outex and VisTex sets, respectively.

The most discriminating color texture feature is:

- the fifth Haralick feature f_5, extracted from the between color component RSCCM $m_{3\times3}^{C_{C1C2},h_{C1C2}}$ computed in the (A,C_{C1C2},h_{C1C2}) perceptual space, for the OuTex texture set,
- the seventh Haralick feature f_7 extracted from the within color component RSCCM $m_{3\times3}^{C'_{UV},C'_{UV}}$ computed in the (Y',C'_{UV},h'_{UV}) perceptual space, for the VisTex set.

We can notice that the inverse difference moment (f_5) is particularly discriminating for the textures since it is selected 8 times out of 20 by the MCSFS approach.

With the 40-dimensional feature sub-space selected by MCSFS, the rate of well-classified validation images reaches:

- **96.6%** for the Outex set,
- **99.8%** for the VisTex set (only one image is misclassified).

These results are higher than those obtained with the SCSS approach (see tables 2 and 3) as we will detail in the next section.

Table 4 The first ten features selected by the MCSFS approach for the Outex set.

d	Color space	RSCCM	Haralick feature
1	(A, C_{C1C2}, h_{C1C2})	$m_{3\times3}^{C_{C1C2},h_{C1C2}}$	inverse difference moment (f_5)
2	(L^*, a^*, b^*)	$m_{3\times3}^{L^*,a^*}$	inverse difference moment (f_5)
3	$(I5, S4, H2)$ or $(I4, S3, H2)$	$m_{3\times3}^{H2,H2}$	sum average (f_6)
4	(r, g, b)	$m_{3\times3}^{b,b}$	sum variance (f_7)
5	(r, g, b)	$m_{3\times3}^{r,b}$	inverse difference moment (f_5)
6	(Y, x, y)	$m_{3\times3}^{Y,x}$	difference variance (f_{10})
7	$(I1, S1, H3)$	$m_{3\times3}^{S1,H3}$	inverse difference moment (f_5)
8	(L^*, a^*, b^*)	$m_{3\times3}^{L^*,b^*}$	inverse difference moment (f_5)
9	(L^*, C^*_{uv}, h_{uv})	$m_{3\times3}^{C^*_{uv},h_{uv}}$	sum average (f_6)
10	$(I4, S3, H2)$	$m_{3\times3}^{S3,H2}$	inverse difference moment (f_5)

Table 5 The first ten features selected by the MCSFS approach for the VisTex set.

d	Color space	RSCCM	Haralick feature
1	(Y', C'_{UV}, h'_{UV})	$m_{3\times3}^{C'_{UV},C'_{UV}}$	sum variance (f_7)
2	(Y', U', V')	$m_{3\times3}^{U',V'}$	inverse difference moment (f_5)
3	(Y', I', Q')	$m_{3\times3}^{I',Q'}$	contrast (f_2)
4	(R, G, B)	$m_{3\times3}^{R,R}$	information measure of correlation (f_{13})
5	$(I4, S3, H2)$	$m_{3\times3}^{S3,S3}$	inverse difference moment (f_5)
6	$(I1, r, g)$ or (r, g, b)	$m_{3\times3}^{g,g}$	sum average (f_6)
7	(A, C_{C1C2}, h_{C1C2})	$m_{3\times3}^{C_{C1C2},C_{C1C2}}$	information measure of correlation (f_{13})
8	(A, C_{C1C2}, h_{C1C2})	$m_{3\times3}^{A,h_{C1C2}}$	contrast (f_2)
9	$(I4, S3, H2)$	$m_{3\times3}^{I4,S3}$	sum entropy (f_8)
10	$(A, C1, C2)$ or (A, C_{C1C2}, h_{C1C2})	$m_{3\times3}^{A,A}$	difference variance (f_{10})

5.4 Accuracy comparison

In order to assess our color texture classification approach, we propose to compare the results that we have obtained with the Outex and VisTex sets with those provided by other authors who have also applied their classification schemes on these sets. To examine more precisely the contribution of the MCSFS approach on the quality of texture classification, we propose to examine different texture features:

- **Luminance**: Haralick features are only computed from gray level co-occurrence matrices. In this case, only the luminance of each pixel is analyzed. The $N_f = 13$ candidate Haralick features extracted from only one gray level co-occurrence matrix are thus taken into account to discriminate the different texture classes.
- **SCSS**: Haralick features are extracted from RSCCMs computed from images whose colors are coded in a single color space ($N_f = 78$). In this case, we evaluate the classification performances obtained by analyzing images coded in the color space for which the SCSS approach has obtained the highest rate of well-classified validation images. This rate is obtained with the $(I5, S4, H2)$ and the $(L, Ch1, Ch2)$ color spaces for the Outex and VisTex sets, respectively (see tables 2 and 3).
- **MCSFS**: Haralick features are extracted from RSCCMs computed from images coded in N_S different color spaces of figure 3 ($N_S = 28$ for the Outex set and $N_S = 20$ for the VisTex set). The feature selection scheme of the MCSFS approach determines the 40-dimensional discriminating feature sub-space from the N_f candidate features ($N_f = 2184$ for the Outex set and $N_f = 1560$ for the VisTex set).
- **MCSWS**: We also propose to directly classify the validation images in the feature space composed of the N_f candidate color texture features, that is to say without performing any selection step. This last approach, called the **Multi Color Space Without Selection (MCSWS) approach**, allows us to evaluate the improvement brought by the feature selection step of the MCSFS approach.

Tables 6 and 7 show the different classification rates reached with the Outex and VisTex validation sub-sets, respectively and sorted in the descending order.

The rows labeled as gray correspond to experiments that are carried out in this paper whereas the other rows correspond to results published by other authors. The considered color spaces used to classify the validation images are presented in the first column of each table. The second column shows the features which have been analyzed to discriminate the different color texture classes. The number Q of levels used to quantize each color component is mentioned. Finally, the last column shows the rate T (%) of well-classified

Table 6 Comparison between the well-classified image rates reached with the Outex validation sub-set.

Color space	Features	Classifier	T (%)
MCSFS	Haralick features from RSCCMs ($Q = 16$)	1-NN	**96.6**
$(I4, S3, H2)$	3D color histogram ($Q = 16$) [2]	1-NN	95.4
(R, G, B)	Haralick features from RSCCMs ($Q = 32$) [25]	5-NN	94.9
(R, G, B)	3D color histogram ($Q = 16$) [44]	3-NN	94.7
Improved-HLS	3D color histogram ($Q = 16$) [45]	1-NN	94.5
MCSWS	Haralick features from RSCCMs ($Q = 16$)	1-NN	93.8
$(I4, S3, H2)$	Between and within LBP histogram [7]	SVM	93.5
SCSS $(I5, S4, H2)$	Haralick features from RSCCMs ($Q = 16$)	1-NN	92.5
(R, G, B)	Between color component LBP histogram [2]	1-NN	92.5
Improved-HLS	Features from autoregressive models + 3D color histogram ($Q = 16$) [45]	1-NN	88.9
(L^*, a^*, b^*)	Features from autoregressive models ($Q = 16$) [45]	1-NN	88.0
(R, G, B)	Within color component LBP histogram [2]	1-NN	87.8
(R, G, B)	Features from wavelet transform [8]	7-NN	85.2
Luminance	Haralick features from RSCCMs ($Q = 16$)	1-NN	76.6

Table 7 Comparison between the well-classified image rates reached with the VisTex validation sub-set.

Color space	Features	Classifier	T (%)
$(I1, I2, I3)$	3D color histogram ($Q = 32$) [2]	1-NN	**100**
(L^*, a^*, b^*)	Within color component LBP histogram [2]	1-NN	**100**
MCSFS	Haralick features from RSCCMs ($Q = 16$)	1-NN	99.8
$(I1, I2, I3)$	3D color histogram ($Q = 16$) [44]	3-NN	99.8
(R, G, B)	Between and within LBP histogram [7]	SVM	99.8
(R, G, B)	Between color component LBP histogram [2]	1-NN	99.5
MCSWS	Haralick features from RSCCMs ($Q = 16$)	1-NN	99.3
SCSS $(L, Ch1, Ch2)$	Haralick features from RSCCMs ($Q = 16$)	1-NN	99.3
(R, G, B)	Haralick features from RSCCMs ($Q = 32$) [25]	5-NN	97.7
Luminance	Haralick features from RSCCMs ($Q = 16$)	1-NN	82.6

validation images obtained with the classifier defined in the third column.

By analyzing these tables, we can notice that the classification results obtained with features extracted from images coded in a single color space largely outperform those obtained with gray level features. This result confirms that that analyzing the color information significantly improves the quality of texture classification.

On the other hand, the accuracy provided by MCSWS approach is higher or equal to that provided by the one provided by SCSS. This shows that combining several color spaces improves the classification results.

Finally, by analyzing the classification results reached by the MCSWS approach with those obtained with the MCSFS approach, we can confirm that the feature selection step of MCSFS allows to improve more the rates of well-classified validation images while notably decreasing the dimension of the feature space.

Let us note that, for the Outex image set, the accuracy obtained by the proposed MCSFS approach ($T = 96.6\%$) is higher than the best classification rate which has been yet obtained with this set by Mäenpää *et al.* with 3D color histograms ($T = 95.4\%$) [2].

As a conclusion, from the classification accuracy standpoint, it is more relevant to select texture features extracted from different color spaces than selecting a color space when the feature set is initially defined. The next section provides the processing time point of view.

5.5 Processing time

This section aims to evaluate the processing time required by the learning and decision stages of the SCSS, MCSFS and MCSWS approaches.

5.5.1 Learning stage

Table 8 compares the processing times required by the learning stage applied to 680 images of the Outex set whose size is 128×128 pixels. These times are obtained by a software written in C language and processed with a PC cadenced at 2.40 GHz with 448 Mb RAM.

During the learning stage, the features are first computed from images that have been coded in several color spaces (see section 4.1). As the number of candidate features is the same for the three approaches, the time required for feature computation is equal (1 681 s). The MCSWS approach does not perform any feature selection step, contrary to SCSS and MCSFS. Its computation time is so limited to 1 681 s. The color space selection step achieved by SCSS classifies

Table 8 Processing time of the learning stage (for 680 training images whose size is 128 × 128 pixels).

	Feature computation	Color space or feature selection	Total
SCSS	1 681 s	112 393 s	114 074 s
MCSWS		–	1 681 s
MCSFS		352 s	2 033 s

the validation images thanks to the 1-NN classifier, that is time consuming. Indeed, its learning stage processing time reaches 114 074 s, that is to say nearly 32 hours. This time is noticeably higher than the MCSFS ones (2 033 s) whose feature selection step follows a filter approach which does not classify the images.

5.5.2 Decision stage

The decision stage is divided into two successive steps: the feature computation and the classification steps.

Table 9 Processing time of the decision stage (for one validation image whose size is 128 × 128 pixels).

	Feature computation	Classification	Total
SCSS	88 ms	5 903 ms	5.99 s
MCSWS	2 472 ms	182 876 ms	185.35 s
MCSFS	45 ms	3 385 ms	3.43 s

Table 9 shows that the processing time required by the 1-NN classifier for classifying an image, whose size is 128 × 128 pixels, is 5.99 s when the SCSS approach is performed, 185.35 s (that is to say 3 minutes and 5 seconds) when the MCSWS approach is computed and 3.43 s when the MCSFS approach is performed.

Tables 6 (accuracy), 8 and 9 (processing times) show that the proposed MCSFS approach allows to obtain better classification results to the SCSS ones, with lower learning and decision processing times. It is thus more relevant to select texture features extracted from different color spaces than selecting a color space, the features being initially retained, from the classification accuracy and processing time points of view.

6 Discussion

These experiments have been achieved with the Outex and VisTex color texture sets which have already been used by several other authors to assess the efficiency of their color texture classification schemes. Tables 6 and 7, which synthesize these works, show that very high classification accuracies are obtained by Mäenpää *et al.* with color histogram on these two sets [2]. However, color histogram only characterizes the color distribution within the color space and does not take into account the spatial relationships between neighboring pixels. To understand the reason why color histogram allows to obtain the best classification results whereas it does not take into account any texture information, let us examine the Outex and VisTex sets.

These sets are divided into two sub-sets: the training and the validation sub-sets. The sub-images which constitute these two sub-sets come from the same original image of color texture according to the decomposition presented in figure 8.

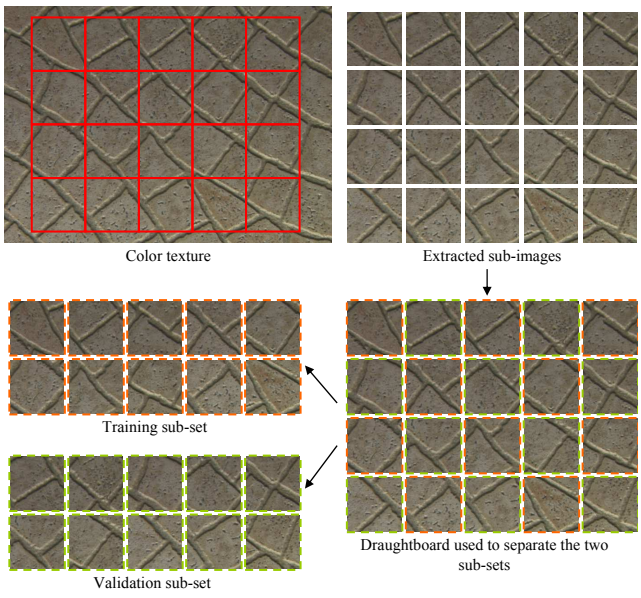

Fig. 8 Building of the training and the validation sub-sets according to a draughtboard decomposition.

This figure shows that ten sub-images extracted from the color texture constitute the training sub-set, while the ten others are the validation images. As the sub-images of the training sub-set and those of the validation one come from the same original color texture image, they are very similar. So, the points which characterize these color texture sub-images should be very close to each other whatever the considered feature space.

Hence, the probability that a 1-NN classifier assigns sub-images coming from the same original image to a same class is very high because, at least one training sub-image is always spatially close to any validation sub-image (see draughtboard decomposition of figure 8). This phenomenon is experimentally verified thanks to the results presented in

tables 10 and 11. Indeed, these tables show the classification rates reached by the 1-NN and the rank sum classifiers for different color texture features. The rank sum classifier first computes the distances between the training images and each validation image in the feature space and then ranks the obtained measures in ascending order. For each class, the sum of rank of its training images is then computed and the validation image is finally assigned to the class for which the rank sum is the lowest. To make the decision, the classifier takes into account all the training images, and even possible outliers like training sub-images which are spatially far from the validation sub-image to be classified. So high accuracy is more difficult to be obtained with the rank sum classifier than with the 1-NN one. The rates of images well-classified by the rank sum thus indicate more precisely the discriminating power of the examined feature spaces.

The color texture features which are computed for this experimental check are described in section 5.4. Furthermore, we also use 3D color histograms that are extracted from a well-suited color space (see tables 6 and 7). As Mäenpää *et al.* do, these histograms are compared thanks to the histogram intersection measure and they are extracted from color texture images coded in the $(I4, S3, H2)$ color space with Q set to 16, for the Outex set and from images coded in the $(I1, I2, I3)$ color space with Q set to 32, for the VisTex set [2] (see tables 6 and 7).

By analyzing tables 10 and 11, we first notice that the rates of well-classified images obtained by the four tested approaches are close when the 1-NN classifier operates, whereas they are scattered when the rank sum classifier is performed. With this last classifier, we note that the accuracy is the lowest when the color histogram is computed or when the SCSS approach operates. Moreover, MCSFS outperforms the other tested approaches. The low dimensional feature sub-space selected by the MCSFS approach is thus the most robust against the used classifier and is the most relevant to classify textures.

These experiments allow us to conclude that training and validation sub-images have to come from different original images in order to ensure that color texture images are less correlated as possible. This decomposition would be besides more consistent with those which are considered in the framework of concrete industrial applications, where the training images are different from the images that are on-line classified.

7 Conclusion

In this paper, we have compared two texture classification strategies that use color spaces: the Single Color Space Selection (SCSS) approach and the Multi Color Space Feature Selection (MCSFS) ones. These approaches, based on a supervised learning scheme, allow to answer the issue that there is no color space which is well-adapted to the discrimination of all texture databases, whatever the considered texture features. The prior determination of a well-suited color space being not easy, the SCSS approach proposes to define a set of texture features and to select the color space with which the texture features reach the highest classification accuracy, whereas the MSCFS scheme selects texture features that have been processed from images coded into different color spaces.

Experimental results have been carried out with two sets of color textures images extracted from well-known and largely used benchmark databases: Outex and VisTex. We have firstly applied the Single Color Space Selection (SCSS) approach to different color spaces and have shown that the classification accuracy strongly depends on the considered color space. Furthermore, we have noticed that extracting features from images coded in a perceptual space allows generally to obtain very satisfying classification results whatever the considered database.

We have then applied the MCSFS approach and have shown that the obtained classification results (**96.6%** for the Outex set and **99.8%** for the VisTex set) are close or even higher than the best classification results which have been yet obtained with the Outex and VisTex sets.

The comparison of the classification performances reached by the SCSS and the MCSFS approaches allows us to conclude that taking advantage simultaneously of the properties of several color spaces tends to improve the rates of well-classified images. We have also seen that the feature selection step allows to more increase these rates while notably decreasing the dimension of the feature space. Finally, we have shown that the processing times of the learning and the decision stages of MCSFS are lower than those consumed by SCSS.

As a conclusion, it is thus more relevant to select texture features extracted from different color spaces than selecting a color space with a set of texture features initially defined, from the classification accuracy and processing time points of view.

Finally, this experimental study has led us to conclude that the examined benchmark image sets are not really efficient to measure the relevance of color texture classification schemes. Indeed, we have noticed that 3D color histogram allows to obtain the best classification results on these color texture sets whereas it does not take into account any spatial information. We have thus shown that the draughtboard decomposition (see figure 8) which has been chosen to built these sets led to biased classification results when the 1-NN classifier is considered. This study shows the necessity to dispose of a color texture set more suitable and more relevant for evaluating the performances reached by color texture classification methods. This set should be built thanks to a specific decomposition where the training and the val-

Table 10 Classification rates reached by the 1-NN and the rank sum classifiers, for the Outex validation sub-set.

Color space	Features	T (%) with 1-NN	T (%) with rank sum
MCSFS	Haralick features from RSCCMs ($Q = 16$)	**96.6**	**90.3**
MCSWS	Haralick features from RSCCMs ($Q = 16$)	93.8	89.3
SCSS $(I5, S4, H2)$	Haralick features from RSCCMs ($Q = 16$)	92.5	82.5
$(I4, S3, H2)$	3D color histogram ($Q = 16$)	95.4	80.7

Table 11 Classification rates reached by the 1-NN and the rank sum classifiers, for the VisTex validation sub-set.

Color space	Features	T (%) with 1-NN	T (%) with rank sum
MCSFS	Haralick features from RSCCMs ($Q = 16$)	99.8	**95.1**
MCSWS	Haralick features from RSCCMs ($Q = 16$)	99.3	94.0
SCSS $(L, Ch1, Ch2)$	Haralick features from RSCCMs ($Q = 16$)	99.3	90.5
$(I1, I2, I3)$	3D color histogram ($Q = 32$)	**100**	82.4

idation sub-images of a same texture come from different original images in order to ensure that color texture images are less correlated as possible.

References

1. C. Palm, "Color texture classification by integrative co-occurrence matrices," *Pattern Recognition Letters*, vol. 37, no. 5, pp. 965–976, 2004.
2. T. Mäenpää and M. Pietikäinen, "Classification with color and texture: jointly or separately?," *Pattern Recognition Letters*, vol. 37, no. 8, pp. 1629–1640, 2004.
3. E.L. Van Den Broek and E.M. Van Rikxoort, "Evaluation of color representation for texture analysis," in *Proceedings of the Belgium-Dutch Conference on Artificial Intelligence*, 2004, pp. 35–42.
4. L. Busin, N. Vandenbroucke, and L. Macaire, *Color spaces and image segmentation*, vol. 51, chapter 2, pp. 65–168, Advances in Imaging and Electron Physics, 2008.
5. G. Van de Wouwer, P. Scheunders, S. Livens, and D. Van Dyck, "Wavelet correlation signatures for color texture characterization," *Pattern Recognition*, vol. 32, pp. 443–451, 1999.
6. M. Singh, M. Markou, and S. Singh, "Colour image texture analysis: Dependence on colour spaces," in *Proceedings of the 16th International Conference on Pattern Recognition*, 2002, vol. 1, pp. 672–676.
7. D. Iakovidis, D. Maroulis, and S. Karkanis, "A comparative study of color-texture image features," in *Proceedings of 12th International Workshop on Systems, Signals & Image Processing (IWSSIP'05), Chalkida, Greece*, 2005, pp. 203–207.
8. Q. Xu, J. Yang, and S. Ding, "Color texture analysis using the wavelet-based hidden markov model," *Pattern Recognition Letters*, vol. 26, pp. 1710–1719, 2005.
9. S. Arivazhagan, L. Ganesan, and V. Angayarkanni, "Color texture classification using wavelet transform," in *Proceedings of the Sixth International Conference on Computational Intelligence and Multimedia Applications (ICCIMA '05)*, 2005, pp. 315–320.
10. P.S. Hiremath, S. Shivashankar, and J. Pujari, "Wavelet based features for color texture classification with application to CBIR," *International Journal of Computer Science and Network Security (IJCSNS)*, vol. 6, no. 9, pp. 124–133, 2006.
11. A. Sengur, "Wavelet transform and adaptive neuro-fuzzy inference system for color texture classification," *Expert Systems with Applications*, vol. 34, no. 3, pp. 2120–2128, 2008.
12. M.A. Akhloufi, X. Maldague, and W.B. Larbi, "A new color-texture approach for industrial products inspection," *Journal of Multimedia*, vol. 3, no. 3, pp. 44–50, 2008.
13. L. Nanni and A. Lumini, "Fusion of color spaces for ear authentication," *Pattern Recognition*, vol. 42, no. 9, pp. 1906–1913, 2009.
14. S. Chindaro, K. Sirlantzis, and F. Deravi, "Texture classification system using colour space fusion," *Electronics Letters*, vol. 41, no. 10, pp. 589–590, 2005.
15. A. Porebski, N. Vandenbroucke, and L. Macaire, "Iterative feature selection for color texture classification," in *IEEE International Conference on Image Processing*, San Antonio, 2007, pp. 509–512.
16. N. Vandenbroucke, L. Macaire, and J.-G. Postaire, "Color image segmentation by pixel classification in an adapted hybrid color space. application to soccer image analysis," *Computer Vision and Image Understanding*, vol. 90, no. 2, pp. 190–216, 2003.
17. T. D'Orazio and M. Leo, "A review of vision-based systems for soccer video analysis," *Pattern Recognition*, vol. 43, no. 8, pp. 2911–2926, 2010.
18. A. Jain and D. Zongker, "Feature selection : evaluation, application and small sample performance," *IEEE Transactions on Pattern Analysis and Machine Intelligence*, vol. 19, no. 2, pp. 153–158, 1997.
19. M. Tuceryan and A.K. Jain, "Texture analysis," in *The Handbook of Pattern Recognition and Computer Vision*. 1998, pp. 207–248, Editions World Scientific Publishing Co.
20. C. Zheng, D.W. Sun, and L. Zheng, "A new region-primitive method for classification of colour meat image texture based on size, orientation and contrast," *Meat Science*, vol. 76, no. 4, pp. 620–627, 2007.
21. A. Khotanzad and O.J. Hernandez, "A classification methodology for color textures using multispectral random field mathematical models," *Mathematical and Computational Applications*, vol. 11, no. 2, pp. 111–120, 2006.
22. O.J. Hernandez, J. Cook, M. Griffin, C. De Rama, and M. McGovern, "Classification of color textures with random field models and neural networks," *Journal of Computer Science & Technology*, vol. 5, no. 3, pp. 150–157, 2005.
23. C. Palm and T.M. Lehmann, "Classification of color textures by gabor filtering," *Machine Graphics & Vision International Journal*, vol. 11, no. 2, pp. 195–219, 2002.
24. A. Drimbarean and P.F. Whelan, "Experiments in colour texture analysis," *Pattern Recognition Letters*, vol. 22, no. 10, pp. 1161–1167, 2001.
25. V. Arvis, C. Debain, M. Berducat, and A. Benassi, "Generalization of the cooccurrence matrix for colour images: application to colour texture classification," *Image Analysis and Stereology*, vol. 23, pp. 63–72, 2004.
26. J. Martinez-Alajarin, J.D. Luis-Delgado, and L.M. Tomas-Balibrea, "Automatic system for quality-based classification of marble textures," *IEEE Transactions on Systems, Man and Cybernetics*, vol. 35, no. 4, pp. 488–497, 2005.

27. C. Münzenmayer, H. Volk, C. Küblbeck, K. Spinnler, and T. Wittenberg, "Multispectral texture analysis using interplane sum- and difference-histograms," in *DAGM-Symposium*. 2002, pp. 42–49, Editions Springer-Verlag.
28. A. Porebski, N. Vandenbroucke, and L. Macaire, "Haralick feature extraction from LBP images for color texture classification," in *First IEEE international Workshops on Image Processing Theory, Tools and Applications*, Sousse, 2008, pp. 1–8.
29. T. Mäenpää, J. Viertola, and M. Pietikäinen, "Optimising colour and texture features for real-time visual inspection," *Pattern Analysis and Applications*, vol. 6, no. 3, pp. 169–175, 2003.
30. F. Lopez, J.M. Valiente, J.M. Prats, and A. Ferrer, "Performance evaluation of soft color texture descriptors for surface grading using experimental design and logistic regression," *Pattern Recognition*, vol. 41, no. 5, pp. 1761–1772, 2008.
31. I.U.H. Qazi, O. Alata, J.C. Burie, and C. Fernandez-Maloigne, "Color spectral analysis for spatial structure characterization of textures in ihls color space," *Pattern Recognition*, vol. 43, no. 3, pp. 663–675, 2010.
32. X. Xie and M. Mirmehdi, "Texems: Texture exemplars for defect detection on random textured surfaces," *IEEE Transactions on Pattern Analysis and Machine Intelligence*, vol. 29, no. 8, pp. 1454–1464, 2007.
33. A. Porebski, N. Vandenbroucke, and L. Macaire, "Selection of color texture features from reduced size chromatic co-occurrence matrices," in *IEEE International Conference on Signal and Image Processing Applications*, Malaysia, 2009, pp. 273–278.
34. A. Rosenfeld, C.Y. Wang, and A.Y. Wu, "Multispectral texture," *IEEE Transactions on Systems, Man and Cybernetics*, vol. 12, no. 1, pp. 79–84, 1982.
35. R. Haralick, K. Shanmugan, and I. Dinstein, "Textural features for image classification," *IEEE Transactions on Systems, Man and Cybernetics*, vol. 3, no. 6, pp. 610–621, 1973.
36. A. Porebski, N. Vandenbroucke, and L. Macaire, "Neighborhood and haralick feature extraction for color texture analysis," in *4th European Conference on Colour in Graphics, Imaging, and Vision*, Terrassa, 2008, pp. 316–321.
37. Y.I. Ohta, T. Kanade, and T. Sakai, "Color information for region segmentation," *Computer Graphics and Image Processing*, vol. 13, pp. 222–241, 1980.
38. K. N. Plataniotis and A. N. Venetsanopoulos, *Color Image Processing and Applications*, Springer, 2001.
39. T. Ojala, T. Mäenpää, M. Pietikäinen, J. Viertola, J. Kyllönen, and S. Huovinen, "Outex new framework for empirical evaluation of texture analysis algorithms," in *Proceedings of the 16th International Conference on Pattern Recognition*, 2002, vol. 1, pp. 701–706.
40. R. Picard, C. Graczyk, S. Mann, J. Wachman, L. Picard, and L. Campbell, "Vision texture database," Media Laboratory, Massachusetts Institute of Technology (MIT), Cambridge, http:// vismod.media.mit.edu/ pub/ VisTex/ VisTex.tar.gz.
41. P. Pudil, J. Novovicova, and J. Kittler, "Floating search methods in feature selection," *Pattern Recognition Letters*, vol. 15, pp. 1119–1125, 1994.
42. A. Porebski, N. Vandenbroucke, and L. Macaire, "Comparison of feature selection schemes for color texture classification," in *Second IEEE international Workshops on Image Processing Theory, Tools and Applications*, Paris, 2010, pp. 32–37.
43. R. Webster, "Wilks's criterion: a measure for comparing the value of general purpose soil classifications," *Journal of Soil Science*, vol. 22, pp. 254–260, 1971.
44. M. Pietikäinen, T. Mäenpää, and J. Viertola, "Color texture classification with color histograms and local binary patterns," in *Proceedings of the 2nd International Workshop on Texture Analysis and Synthesis*, 2002, pp. 109–112.
45. I.U.H. Qazi, O. Alata, J.C. Burie, and A. Moussa C. Fernandez-Maloigne, "Choice of a pertinent color space for color texture characterization using parametric spectral analysis," *Pattern Recognition*, vol. 44, no. 1, pp. 16–31, 2011.